

RESEARCH

Open Access



Texture analysis of cardiovascular MRI native T1 mapping in patients with Duchenne muscular dystrophy

Mary Luz Mojica-Pisciotti¹ , Tomáš Holeček^{2,3*} , Věra Feitová⁴ , Lukáš Opatřil⁵ and Roman Panovský⁵

Abstract

Background Duchenne muscular dystrophy (DMD) patients are monitored periodically for cardiac involvement, including cardiac MRI with gadolinium-based contrast agents (GBCA). Texture analysis (TA) offers an alternative approach to assess late gadolinium enhancement (LGE) without relying on GBCA administration, impacting DMD patients' care. The study aimed to evaluate the prognostic value of selected TA features in the LGE assessment of DMD patients.

Results We developed a pipeline to extract TA features of native T1 parametric mapping and evaluated their prognostic value in assessing LGE in DMD patients. For this evaluation, five independent TA features were selected using Boruta to identify relevant features based on their importance, least absolute shrinkage and selection operator (LASSO) to reduce the number of features, and hierarchical clustering to target multicollinearity and identify independent features. Afterward, logistic regression was used to determine the features with better discrimination ability. The independent feature inverse difference moment normalized (IDMN), which measures the pixel values homogeneity in the myocardium, achieved the highest accuracy in classifying LGE (0.857 (0.572–0.982)) and also was significantly associated with changes in the likelihood of LGE in a subgroup of patients with three yearly examinations (estimate: 23.35 (8.7), p-value = 0.008). Data are presented as mean (SD) or median (IQR) for normally and non-normally distributed continuous variables and numbers (percentages) for categorical ones. Variables were compared with the Welch t-test, Wilcoxon rank-sum, and Chi-square tests. A P-value < 0.05 was considered statistically significant.

Conclusion IDMN leverages the information native T1 parametric mapping provides, as it can detect changes in the pixel values of LGE images of DMD patients that may reflect myocardial alterations, serving as a supporting tool to reduce GBCA use in their cardiac MRI examinations.

Keywords Cardiac MRI, Texture analysis, Duchenne muscular dystrophy, Radiomics

*Correspondence:

Tomáš Holeček
tomas.holecek@fnusa.cz

¹International Clinical Research Center, St. Anne's University Hospital, Pekařská 53, 60200 Brno, Czech Republic

²International Clinical Research Center and Department of Medical Imaging, St. Anne's University Hospital, Faculty of Medicine, Masaryk University, Pekařská 53, Brno 602 00, Czech Republic

³Department of Biomedical Engineering, Brno University of Technology, Technická 3082, 60200 Brno, Czech Republic

⁴International Clinical Research Center and Department of Medical Imaging, St. Anne's University Hospital, Pekařská 53, 60200 Brno, Czech Republic

⁵International Clinical Research Center and 1st Department of Internal Medicine/Cardioangiology, St. Anne's University Hospital, and Faculty of Medicine, Masaryk University, Pekařská 53, 60200 Brno, Czech Republic



© The Author(s) 2025. **Open Access** This article is licensed under a Creative Commons Attribution 4.0 International License, which permits use, sharing, adaptation, distribution and reproduction in any medium or format, as long as you give appropriate credit to the original author(s) and the source, provide a link to the Creative Commons licence, and indicate if changes were made. The images or other third party material in this article are included in the article's Creative Commons licence, unless indicated otherwise in a credit line to the material. If material is not included in the article's Creative Commons licence and your intended use is not permitted by statutory regulation or exceeds the permitted use, you will need to obtain permission directly from the copyright holder. To view a copy of this licence, visit <http://creativecommons.org/licenses/by/4.0/>. The Creative Commons Public Domain Dedication waiver (<http://creativecommons.org/publicdomain/zero/1.0/>) applies to the data made available in this article, unless otherwise stated in a credit line to the data.

Background

Duchenne muscular dystrophy (DMD) is a severe X-linked genetic disease that affects predominantly males (carrier females may also exhibit subtle myocardial changes), generating progressive muscle deterioration and severe motor impairments [1]. Considering their risk for developing cardiac pathologies [1], sufferers must be periodically examined for cardiac involvement, typically once yearly [2]. Their screening starts at a young age and might include cardiac magnetic resonance imaging (MRI) to characterize their myocardial tissue and evaluate and monitor their cardiac health [1–4]. This imaging modality encompasses advanced techniques, such as native T1 parametric mapping, which quantifies the longitudinal relaxation time and provides detailed information about tissue composition [5, 6], and late gadolinium enhancement (LGE), which assesses myocardial tissue and requires the use of gadolinium-based contrast agents (GBCA) [7, 8].

Even though LGE is highly reproducible, it may not be suitable for patients with renal impairment, as it has been shown that GBCA deposition, though without substantial clinical effects, may be associated with the development of nephrogenic systemic fibrosis (NSF) in this group [9–14]. Moreover, other effects of GBCA in different populations, such as gadolinium retention in the central nervous system [15], nonuniform deposition in the brain [9, 16], and mild and moderate adverse reactions have been reported [17]. Nonetheless, the adverse effects of GBCA use are an active research topic.

So far, no studies have focused on GBCA deposition specifically in DMD patients, although concerns about their general long-term safety persist [18, 19], including the need for a more conservative approach to GBCA use in those with documented LGE [20]. It has also been reported that DMD patients might be at risk of developing kidney impairment due to the nature of the disease [19], even in advanced stages [21], meaning that in such cases, GBCA administration may need to be avoided due to the risk of NSF and potential deposition effects. An additional but less frequently addressed concern, despite its clinical relevance, is the administration of GBCA in DMD patients with difficult intravenous access. Although different techniques are proposed in the literature to face this challenge in broader contexts [22], in DMD sufferers, it often requires multiple attempts and is not always successful, indicating that non-contrast cardiac MRI may be more suitable for these cases where GBCA administration is not possible or is contraindicated [4, 20]. Therefore, minimizing the need for contrast use while maintaining the diagnostic accuracy of cardiac MRI remains a critical challenge [20, 23]. DMD patients might benefit from alternative approaches, including

computational-based ones, to fully take advantage of the diagnostic potential of native cardiac MRI methods.

A step towards reducing GBCA use in cardiac MRI in DMD patients is the application of texture analysis (TA), a radiomics-based technique focused on mining data contained in images to quantify features that allow the extraction of information about tissues' underlying structure and possibly function [24–27]. Its application in MRI for several cardiac pathologies has increased lately [27–36], as it could promote a strategic shift toward a safer and more effective approach for yearly cardiac MRI controls. In DMD patients, TA could improve the capability of T1 parametric mapping to detect diffuse myocardial alterations, enhancing its diagnostic value. While alternative radiomics-based approaches exist [24, 25, 37], TA quantifies image heterogeneity, possibly correlating with fibrosis and microstructural changes [24, 25].

This study was necessary to explore the impact of TA in native T1 parametric mapping as a contrast-free, computational approach to assess LGE in DMD patients, addressing the need to reduce the use of GBCA in their monitoring, given the potential risks associated with repeated contrast exposure.

Methods

We hypothesize that TA features extracted from cardiac MRI parametric native T1 maps can provide information about LGE in DMD patients, potentially reducing the need to use GBCA in their yearly controls. Therefore, this study aims to evaluate the prognostic value of selected TA features in the LGE assessment of DMD patients.

Study population

We retrospectively included 67 patients diagnosed with DMD and analyzed the first cardiac MRI examination at the start of their regular screening. Fifteen were randomly selected and reserved for the first step of the study. The remaining patients with complete examinations, i.e., with LGE data (LGE+ and LGE-), were matched by age using optimal full matching with a logistic regression model to estimate the probability of LGE status [38, 39]. This approach creates subclasses that minimize age differences, resulting in balanced groups for comparison. Exams without LGE images corresponded to examinations where inserting the intravenous contrast bolus was not possible because of difficult venous access.

The cardiac MRI examinations were performed from December 1st, 2016, to December 2nd, 2022. These patients were earlier screened by the Parent Project from the Czech Republic [40–43] following the principles from the Declaration of Helsinki (2000) by the World Medical Association. The institutional ethics committee at the Hospital approved the original study (reference number blinded for review). All participants had written

informed consent from their legally authorized representatives or the subjects themselves. Their clinical data was retrieved from the Hospital Information System.

Cardiac MRI data acquisition

Cardiac MRI studies were performed on a 1.5 T scanner (Ingenia, Philips Medical Systems) following a standard protocol [44]. Long-axis and short-axis cine images were acquired with balanced turbo field echo steady-state free precession (SSFP) sequences. T1 parametric mapping was performed at the mid-ventricular level in the short-axis orientation using a modified Look-Locker inversion recovery sequence (MOLLI) before and 15 min after a contrast bolus injection [0.2 mmol/kg, gadobutrol (Gadovist, Bayer)]. MOLLI acquisition schemas of 5(3)3 and 4(1)3(1)2 were used for native and post-contrast T1 maps, respectively.

Finally, LGE images were acquired approximately 10 min after the contrast bolus injection with an inversion-recovery turbo field echo (IR-TFE) sequence, revealing contrast-enhanced areas in both long- and short-axis views. Typical parameters for selected cardiac MRI sequences in the protocol are listed in Table 1.

Clinical assessment

An expert radiologist performed the clinical assessment according to the established clinical protocols [45] using the IntelliSpace Portal (ISP) workspace (version 11, Philips Healthcare). Quantitative assessment of the left ventricular (LV) and right ventricular (RV) functions was described through the ejection fraction (EF), end-diastolic volume (EDV), end-systolic volume (ESV), stroke volume (SV), and cardiac output (CO). The assessment

used cine images and also included the LV mass (LVM), tricuspid annular plane systolic excursion (TAPSE), mitral annular plane systolic excursion (MAPSE), and RV wall thickness (RVWT). LV and RV volumes were indexed to the body surface area (BSA), indicated at the end of the abbreviations with the letter I. Two clinical experts assessed LGE by identifying an area of contrast enhancement where the signal was higher than the mean signal intensity of a reference myocardium zone.

Cardiac MRI T1 mapping assessment

Using the commercial software cvi42 (release 5.13.9, Circle Cardiovascular Imaging, Calgary, Canada), two experienced readers performed T1 parametric mapping assessments. The readers were blinded to the personal and clinical data. They traced the endocardial and epicardial contours in a mid-ventricular slice, excluding the trabeculae and the myocardial blood pool. Then, they verified the alignment in each slice and registered the images with a contour-based registration method. Finally, they generated and exported the motion-corrected native T1 maps for further analysis.

Texture analysis

A successful pipeline was developed to perform the texture analysis in all patients using PyRadiomics (v3.1.0) [46] and Python (v3.7.16). DICOM images of motion-corrected native T1 maps were converted to NIfTI (Neuroimaging Informatics Technology Initiative) format for further processing. The corresponding myocardial mask, i.e., the endocardial and epicardial contours, was obtained with an in-house algorithm that extracted contour coordinates and mapped them onto the native T1 map image. The images were resampled to 1.17×1.17 mm to ensure consistency.

TA was performed on the original images with intensities normalized between $\mu \pm 3\sigma$ (μ , the mean value of the gray levels inside the myocardium, and σ , the standard deviation) [47] without and with different filters: gradient filter, square filter, local binary pattern filters with 8 points and radius 1 and 2 (LBP(8,1) and LBP(8,2), respectively), and 2D discrete wavelet low- and high-frequency sub-bands filters (LL, LH, HL, HH).

Texture feature selection

Feature selection started by identifying highly reproducible features by the inter-rater reliability through the intraclass correlation coefficient (ICC) and the coefficient of variation (CV). Two readers independently analyzed 15 randomly selected studies, and one repeated the analysis one month later. These studies were removed from the primary dataset to minimize potential data dependencies. Features with both intra- and interobserver

Table 1 Cardiac MR imaging protocol typical parameters

Parameter	Cine SSFP	MOLLI	LGE
Field of view (mm)	300×300	300×300	319×319
Acquisition voxel size (mm)	1.67×1.67×8.00	2.00×2.00×10.00	1.60×1.75×10.00
Reconstruction matrix	256×256	256×256	288×288
SENSE factor	1.5	2.0	2.5
Cardiac phases per RR interval	30 to 50	-	-
TE/TR	1.71/3.4	0.91/2.0	1.24/4.0
Bandwidth (Hz)	1102.3	1082.0	304.9
Flip angle	60°	35°	15°

Abbreviations: late gadolinium enhancement, LGE; modified Look-Locker inversion recovery sequence, MOLLI; sensitivity encoding, SENSE; steady-state free precession, SSFP; echo time, TE; repetition time, TR

$ICC \geq 0.75$ and $CV \leq 10\%$ were selected for further analysis [29, 48].

The dataset was randomly split into training (67%) and testing (33%) cohorts, and the classes were balanced to ensure the same number of LGE+ and LGE- cases. To further reduce the dimension, two selection algorithms were independently applied to the highly reproducible features data from the training cohort: Boruta, which performs a top-down search to identify relevant features according to their importance [49], and least absolute shrinkage and selection operator (LASSO) with fivefold cross-validation, which reduces features by penalizing the coefficients of the less important ones [50]. The predictors were scaled before running the Boruta selection algorithm to minimize the risk of overfitting, ensuring that all features contributed equally to the model. Using both Boruta and LASSO as complementary algorithms helped ensure that the set of features was consistently identified across different approaches, enhancing the robustness of the feature selection process. Afterward, hierarchical clustering was applied to all variables selected by Boruta and LASSO target multicollinearity and identify independent features, which were compared between the LGE subgroups.

Texture feature analysis

Multiple logistic regression models were trained with each independent feature to identify the features with better discrimination ability. 10-fold cross-validation was performed within each model. The Akaike Information Criterion (AIC) was used to select the best model. All the features were z-score normalized. A decision tree model based on the identified features was applied to determine a set of rules to discriminate for the presence of LGE.

Once significant features were identified, those were extracted for a subgroup of 15 DMD patients from the original cohort with at least three consecutive yearly examinations to assess their influence on the likelihood of having LGE. These were chosen to coincide with changes in LGE status if the patient exhibited it and to minimize bias. A general linear mixed-effects (GLM) model fitted by maximum likelihood (Laplace approximation) was used to study the influence of these features on the presence of LGE by calculating the log odds of LGE occurrence based on the identified features from the first-year native T1 maps.

Statistical analysis

Descriptive statistics are reported as the mean (standard deviation, SD) or median (interquartile range, IQR) for normally and non-normally distributed continuous variables, respectively, and as numbers (percentages) for categorical ones. The normality of the data was checked by the Shapiro-Wilk test and visual inspection of the

histograms. Proportions of categorical variables were analyzed using the Chi-square test of independence. The Welch two-sample t-test and Wilcoxon rank-sum test were used to compare normally and non-normally distributed variables. The adjusted P-value was obtained by using a false discovery rate correction. A P-value < 0.05 was considered statistically significant. The sample size was determined conservatively assuming Cohen's $d = 0.9$, a large but realistic effect size in clinical studies, to achieve a power of 0.8 with a significance level of 0.05. Correlations were calculated using Pearson or Spearman for normally and non-normally distributed variables. The intraobserver and interobserver agreement was assessed with the ICC (type C, two-way mixed-effects model) was determined from fifteen randomly selected cases analyzed by two readers, one of whom repeated them one month apart. The repeatability was classified as poor (< 0.5), fair (0.50 to 0.75), good (0.75 to 0.90), and excellent (0.90 to 1) [51]. The CV was determined as the standard deviation and mean CV ratio. The Variance Inflation Factor (VIF) was determined to assess the multicollinearity of the final independent selected features.

Logistic regression models with 10-fold cross-validation were fitted and compared using the Akaike Information Criterion (AIC) to estimate the probability of a binary outcome. Cohen's kappa was determined to quantify the level of agreement between observed and predicted classifications. Receiver operating characteristic (ROC) analyses were performed to assess the performance of the classification models. The area under the curve (AUC) was reported along with 95% confidence intervals (CI) to quantify the uncertainty of the estimates. Accuracy, balanced accuracy, and F1 score were also determined to evaluate each model's predictive ability.

Longitudinal data analysis was conducted to examine changes in the independent feature with the highest classification accuracy over time for each patient with a generalized linear mixed (GLM) model fitted with maximum likelihood estimation with Laplace approximation. The GLM assessed the influence of the feature on the log odds of LGE presence. The model's fit was evaluated using AIC and Bayesian Information Criterion (BIC). All statistical analyses were performed with R-4.3.0 and RStudio IDE (2023.03.0 + 386, RStudio, PBC), using base R [52], Boruta (v8.0.0, for Boruta selection) [49], brglm (v0.7.2, for fitting generalized linear models with bias-reduced estimators) [53], caret (v6.0-94, for machine learning algorithms and tools) [54], glmnet (v4.1-8, for fitting generalized linear models with elastic net regularization) [55, 56], ICC (v2.4.0, for calculating intraclass correlation coefficients) [57], MatchIt (v4.5.5, for propensity score matching) [38], and pROC (v1.18.5, for analyzing ROC curves and calculating AUC) [58].

Results

Study group

Fifteen cardiac MRI studies were used for identifying highly reproducible features, and 52 for the primary analysis. Forty-eight examinations had LGE assessment, the remaining four corresponded to examinations performed

on DMD patients with difficult peripheral venous access. Patients with and without LGE (LGE+ and LGE-, respectively) were matched by age, and 42 remained for further analyses, 23 LGE+ and 19 LGE-. The LGE patterns were intramural (12 patients), subepicardial (7 patients), and transmural (4 patients). The study flowchart is shown in

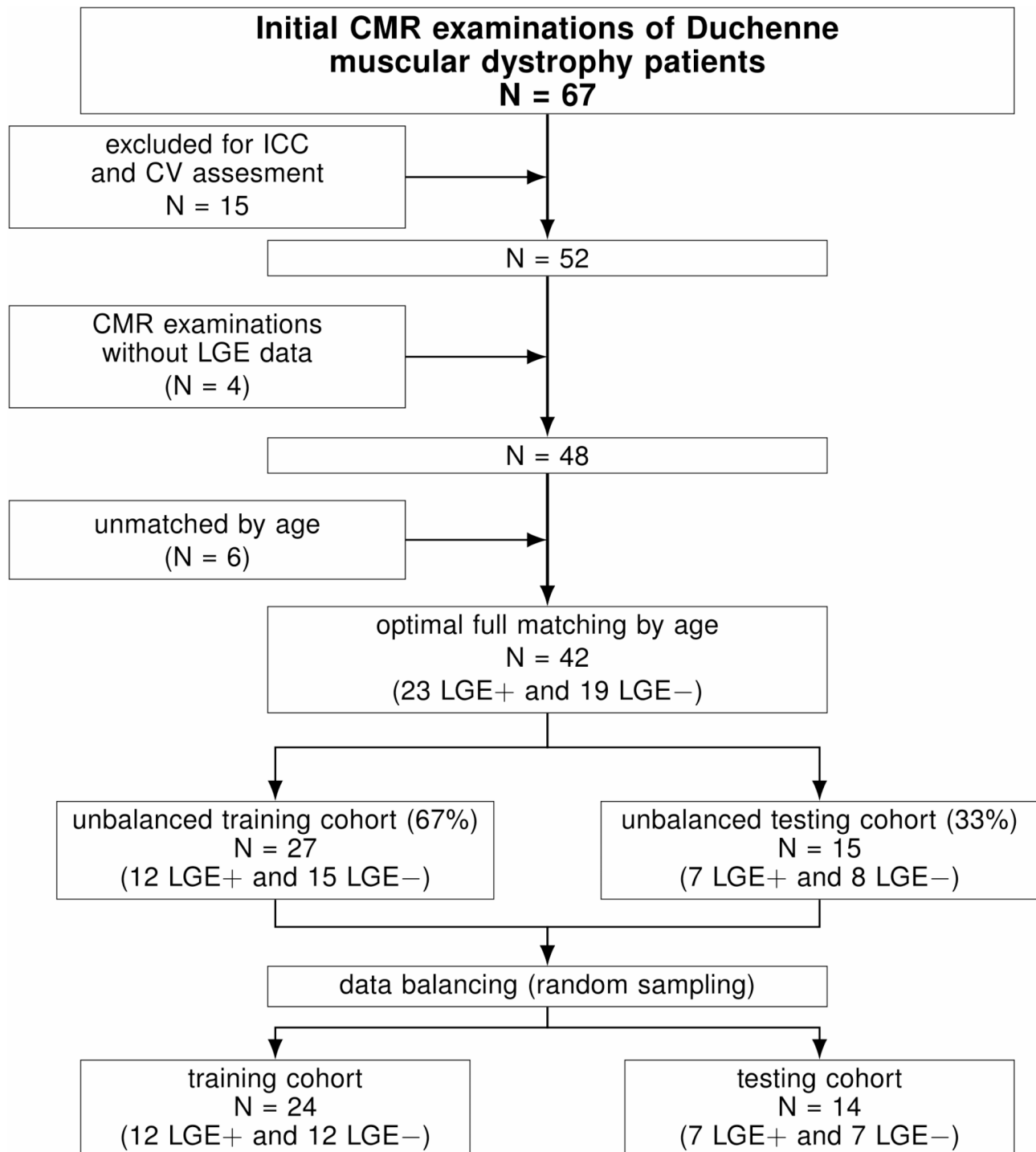


Fig. 1 Study flowchart

Table 2 General characteristics and left and right ventricular function between DMD patients according to LGE

Variable	LGE-, N=19	LGE+, N=23	p-value
Age (y)	12.6 (3.3)	13.8 (3.4)	0.256
BMI (kg/m ²)	21.0 (5.2)	23.6 (6.0)	0.138
BSA (m ²)	1.24 (1.04, 1.45)	1.31 (1.16, 1.63)	0.220
HR (bpm)	95 (11)	100 (15)	0.241
LVEF (%)	69 (64, 76)	58 (51, 66)	0.001
LVEDVI (ml/m ²)	55.3 (41.0, 58.2)	52.6 (46.2, 62.7)	0.468
LVESVI (ml/m ²)	15.2 (12.5, 20.5)	20.4 (16.2, 28.5)	0.014
LVSVI (ml/m ²)	35.7 (8.3)	32.0 (7.0)	0.130
LVMl (g/m ²)	36.6 (30.8, 38.4)	42.8 (35.8, 47.2)	0.015
MAPSE IVS (mm)	11.21 (1.78)	10.07 (1.51)	0.033
MAPSE FW (mm)	11.11 (1.73)	10.41 (2.10)	0.249
MAPSE (average) (mm)	11.16 (1.47)	10.24 (1.51)	0.054
RVEF (%)	67 (64, 74)	63 (52, 70)	0.065
RVEDVI (ml/m ²)	53.8 (12.2)	47.5 (11.0)	0.091
RVESVI (ml/m ²)	17.4 (14.2, 19.7)	17.4 (11.7, 21.4)	0.841
RVSVI (ml/m ²)	34.1 (10.5)	30.0 (7.3)	0.156
TAPSE (mm)	18.0 (3.5)	17.8 (3.3)	0.823
RVWT (mm)	2.00 (2.00, 2.00)	2.00 (2.00, 2.12)	0.124

Variables are expressed as mean (standard deviation) or median (interquartile range) for normally distributed and non-normally distributed continuous variables. Abbreviations: BMI, body mass index; BSA, body surface area; DMD, Duchenne muscular dystrophy; LV, left ventricle; EF, ejection fraction; EDV, end-diastole volume; ESV, end-systole volume; FW, free wall; HR, heart rate; I, indexed; IVS, interventricular septum; LGE, late gadolinium enhancement; LVM, left ventricular mass; MAPSE, mitral annular plane systolic excursion; RV, right ventricle; SV, stroke volume; TAPSE, tricuspid annular plane systolic excursion; WT, wall thickness

Table 3 Cardiac MRI native T1 mapping for DMD patients according to LGE

Variable	LGE-, N=19	LGE+, N=23	p-value
T1 native (ms)			
S1 - Anterior	1016 (1006, 1035)	1053 (1019, 1068)	0.035
S2 - Anteroseptal	1020 (1004, 1041)	1027 (1016, 1052)	0.280
S3 - Inferoseptal	1022 (33)	1037 (35)	0.186
S4 - Inferior	1022 (992, 1045)	1035 (998, 1059)	0.200
S5 - Inferolateral	1032 (48)	1056 (78)	0.218
S6 - Anterolateral	1022 (41)	1042 (53)	0.195
Global	1032 (1002, 1041)	1044 (1013, 1059)	0.065

Variables are expressed as mean (standard deviation) or median (interquartile range) for normally and non-normally distributed continuous. Abbreviations: DMD, Duchenne muscular dystrophy; LGE, late gadolinium enhancement; S, segment

Fig. 1. The participant characteristics are listed in Table 2. Patients without LGE had significantly higher LVEF than those with LGE, although it was preserved in both groups.

Cardiac MRI T1 mapping

The cardiac MRI native T1 mapping analysis is shown in Table 3. The native T1 longitudinal relaxation time significantly differed for the anterior segment between DMD patients according to their LGE status. An example

of native T1 maps and LGE images for two patients is shown in Fig. 2.

Texture analysis

We obtained 918 features per case, including 9 shape-related features, 18 first order, 24 Gy-level co-occurrence matrix (GLCM), 14 Gy-level dependence matrix (GLDM), 16 Gy-level run length matrix (GLRLM), 16 Gy-level size-zone matrix (GLSZM), and 5 neighbouring gray-tone-difference matrix (NGTDM). The description and feature names are shown in Supplementary Table S1. The analysis took 11.68 ± 7.22 s per patient in an Intel(R) Core(TM) i7-8550U CPU @ 1.80 GHz. The results of all texture features were exported for further processing.

Texture feature selection

Of the 918 features, 62 were highly reproducible ones. The group of 42 patients (23 LGE+ and 19 LGE-) was randomly split into training (15 LGE+ and 12 LGE-) and testing (8 LGE+ and 7 LGE-). After balancing the classes, 24 patients remained in the training and 14 in the testing cohorts. The Boruta algorithm selected 20 features using the training cohort; the corresponding importance plot is shown in Supplementary Fig. 1. The Lasso algorithm selected 11 features; the relative feature importance is shown in Supplementary Fig. 2. Three of the identified features were common to both methods, as each selection method focuses on different data patterns: Boruta captures overall importance, while Lasso emphasizes individual associations with the outcome.

Afterward, five features were identified as independent after a hierarchical clustering algorithm was applied: two first-order (root mean squared (RMS)) with filter LBP (8,1) and entropy), two gray-level co-occurrence matrix (inverse difference moment normalized (IDMN) with filter wavelet LL and sum entropy with filter gradient), and one gray-level size-zone matrix (zone%) with filter LBP (8,1). Specifically, RMS is the square root of the mean of all the squared pixel values and measures the magnitude of the image, entropy quantifies the unpredictability of the image's pixel values, IDMN measures the homogeneity of the pixel values, sum entropy quantifies the cumulative variation of pixel intensities across neighbouring pixels, and zone% measures the roughness or coarseness of the texture by zones in the region of interest [46]. The Variance Inflation Factor (VIF) was less than 5 in all cases (see Supplementary Table S2).

Finally, four selected features significantly differed for DMD patients with and without LGE: IDMN, entropy, zone%, and sum entropy. Their comparison is shown in Table 4; Fig. 3.

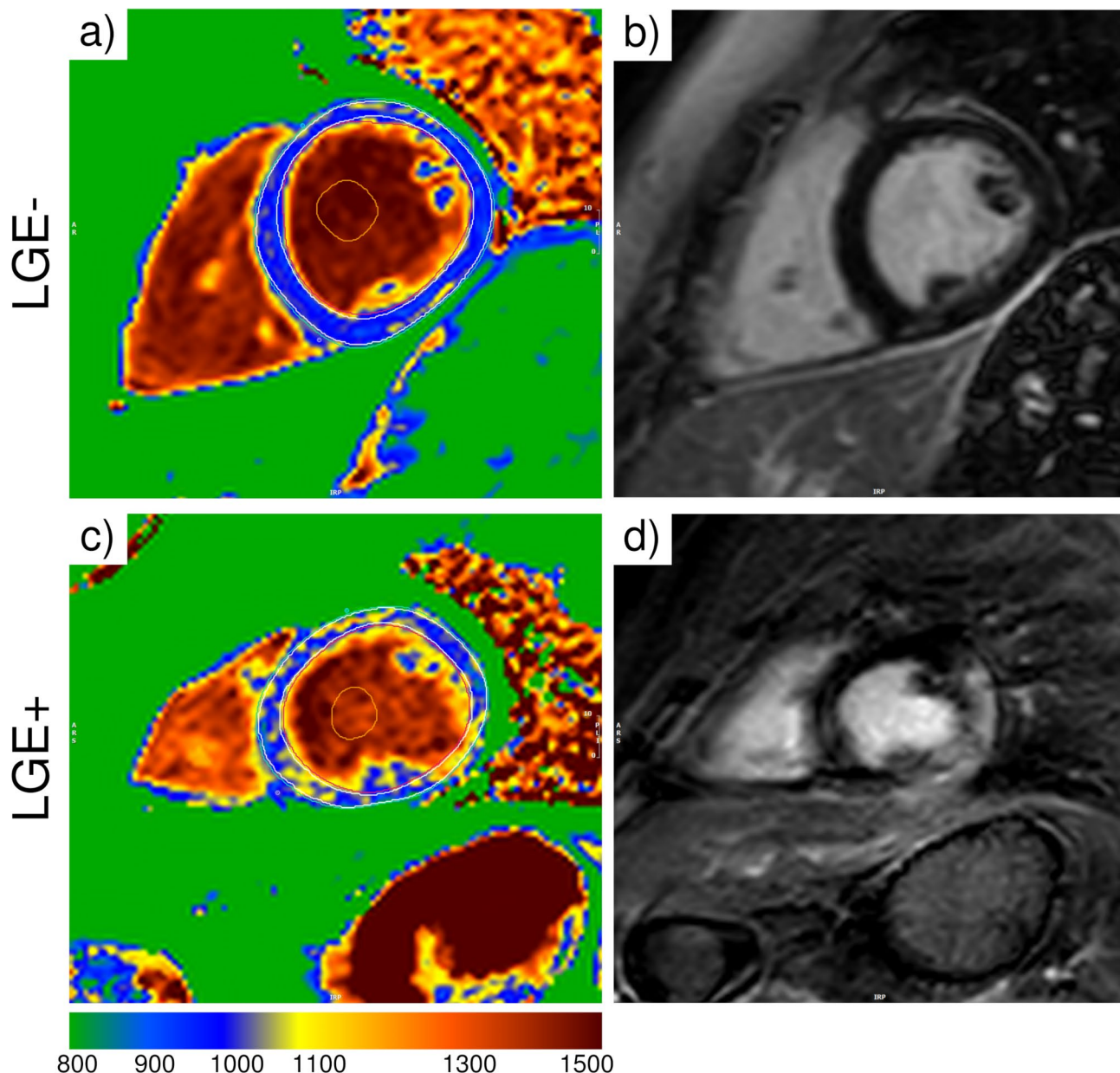


Fig. 2 Representative native T1 maps and late gadolinium enhancement (LGE) images. Panels: **a)** native T1 map for the LGE- patient; **b)** LGE image for the LGE- patient; **c)** native T1 map for the LGE+ patient; **d)** LGE image for the LGE+ patient

Texture feature analysis

The logistic regression model with the IDMN feature achieved the highest accuracy in classifying the samples (accuracy 0.857 (0.572–0.982)) compared to the other significant features, as shown in Table 5. The area under the ROC curve (AUC) for the model with IDMN was 0.889 (95% CI: 0.721, 0.996), indicating good discriminative ability. Additionally, when adjusting models with up to two features, no improvement in accuracy or other metrics was observed. Also, for such a small size, using models with more than two features compromises

statistical reliability and overfitting, making using single features a more viable approach for this analysis.

A decision tree classifier was trained, and an optimal threshold of 0.969 for the IDMN feature was determined for classifying the presence of LGE. Such a choice achieved good discriminative ability (accuracy 0.857 (0.571, 0.982)). The AUC was 0.887 (95% CI: 0.643, 0.995), indicating strong LGE classification performance.

Afterward, the IDMN feature was extracted for a subgroup of 15 DMD patients with at least three consecutive yearly examinations for a preliminary evaluation. A significant effect of IDMN on the log odds of LGE was

Table 4 Comparison of texture features in DMD patients according to LGE

Variables	Type	Filter	LGE-, N= 12	LGE+, N= 12	p-value
IDMN	GLCM	wavelet LL	0.954 (0.009)	0.972 (0.007)	<0.001
Entropy	First order	-	5.07 (4.98, 5.22)	5.28 (5.20, 5.31)	<0.001
Zone%	GLSZM	LBP(8,1)	0.65 (0.03)	0.60 (0.03)	<0.001
RMS	First order	LBP(8,1)	5.66 (0.31)	5.72 (0.29)	0.636
Sum entropy	GLCM	gradient	6.53 (0.20)	6.80 (0.34)	0.025

Variables are expressed as mean (standard deviation) or median (interquartile range) for normally and non-normally distributed continuous. Abbreviations: DMD, Duchenne muscular dystrophy; GLCM, gray-level co-occurrence matrix; GLSZM, gray-level size-zone matrix; IDMN, inverse difference moment normalized; LBP, local binary pattern; LL, low-low; RMS, root mean squared

found (estimate: 23.35 (8.7), p-value=0.008). The GLM showed a good fit to the data (AIC 33.8, BIC 42.6, and log-likelihood - 11.9).

Discussion

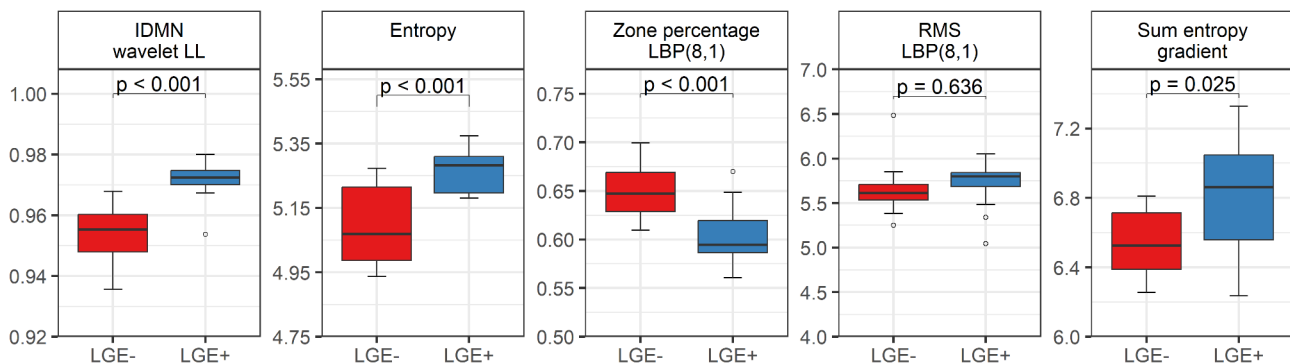
In this work, we studied the added value of texture features extracted from native T1 mapping on LGE assessment in DMD patients. Our findings suggest that one of four features, IDMN or inverse difference moment normalized, is a good option for such a purpose. In the study context, this feature measures the uniformity of the pixel intensity levels within the myocardium in native T1 maps [46]. It plays a crucial role in refining the spatial variations in pixel values derived from T1 parametric

mapping. Therefore, it might help to detect slight alterations where regions with LGE typically exhibit distinct intensity patterns compared to healthy tissue, such as those reported in fibrosis or inflammation [5, 6], without using GBCA.

Texture analysis

Native T1 mapping provides valuable information about myocardial tissue [5, 6], and our results suggest that including IDMN in the assessment might offer a distinct advantage. It enhances the sensitivity of T1 mapping in identifying myocardial alterations and is a non-invasive approach to detect early signs of disease progression. Furthermore, the IDMN feature used the wavelet low-low filter, which focuses on capturing the low-frequency components of the image, emphasizing the broader patterns and textures present in the cardiac MRI native T1 maps while reducing the influence of finer details and noise.

Texture analysis (TA) of native T1 mapping has been used to identify and classify hypertrophic cardiomyopathy [29, 32], diagnose acute myocarditis [28], study heart failure [34], and even characterize diffuse fibrosis patterns [59]. However, to our knowledge, this is the first study focusing on TA in DMD patients intending to impact the use of GBCA in their yearly clinical examinations. As cardiac MRI examinations already pose a challenge for some DMD patients, limiting the time they spend inside the scanner and minimizing GBCA use in this pediatric population would be optimal for detecting

**Fig. 3** Distribution of selected feature values for DMD patients with and without LGE. Abbreviations: IDMN, inverse difference moment normalized; LBP, local binary pattern; LL, low-low; RMS, root mean squared**Table 5** Performance metrics for models with significant features identified by TA and global native T1

Model	Accuracy (95% CI)	AUC (95% CI)	Balanced accuracy	Kappa	F1 Score	AIC
IDMN	0.857 (0.572, 0.982)	0.889 (0.721, 0.996)	0.857	0.714	0.875	18.6
Entropy	0.786 (0.492, 0.953)	0.792 (0.583, 0.995)	0.786	0.571	0.800	22.6
Zone%	0.643 (0.351, 0.872)	0.675 (0.425, 0.896)	0.643	0.286	0.706	26.6
Sum entropy	0.643 (0.351, 0.872)	0.646 (0.396, 0.871)	0.643	0.286	0.667	31.6
Native T1 global	0.571 (0.289, 0.823)	0.578 (0.313, 0.830)	0.571	0.143	0.625	34.3

Variables are expressed as mean (standard deviation) or median (interquartile range) for normally and non-normally distributed continuous. Abbreviations: CI, confidence interval; IDMN, inverse difference moment normalized

early myocardial involvement [3, 12, 20]. Moreover, TA has potential value for patients where administering contrast agents is not feasible, such as in cases with difficult venous access or identification, patient discomfort, anatomical positions that hinder catheter insertion, and potential vascular fragility or compromised circulation associated with DMD.

Native T1 parametric mapping

It has been shown that DMD patients have higher native T1 relaxation times than healthy subjects, regardless of myocardial fibrosis assessed by LGE [43, 60–62]. However, there are contradictory reports regarding identifying LGE status from native T1 maps when comparing DMD patients with and without LGE [43, 60, 61, 63, 64]. Studies found similar values in the segmental and global native T1 relaxation times [43], higher values for LGE+DMD patients limited to the lateral wall [60, 61] or the global assessment [60, 63], and even lower values for LGE+DMD patients compared to those without LGE [64]. We also found higher but not significant global native T1 relaxation times between patients with and without LGE. LVEF was preserved in all DMD, regardless of LGE status, as shown in other studies [65].

These contradictory results regarding native T1 relaxation times might benefit from adding an extra layer of detail, considering also that a previous study showed that, by itself, native T1 parametric mapping is not a strong predictor of LGE in DMD [18]. From our findings, IDMN leverages the information in T1 parametric mapping, refining the spatial variations in the pixel values and identifying subtle alterations in tissue texture. As a result, it might complement the utility of native T1 mapping in identifying potential LGE in DMD patients without using GBCA. Furthermore, we found a significant effect on the logs of LGE by a preliminary assessment of this feature over time, suggesting that IDMN has a strong potential to help predict LGE progression in DMD patients, and monitoring this feature could also help reduce the frequency of GBCA use in their cardiac MRI examinations.

Finally, the clinical relevance of our study lies in the potential of TA to complement native T1 parametric mapping in DMD patients, considering the challenges they might experience during cardiac MRI examinations [20]. Even though only four of our participants had difficult peripheral venous access, this issue is commonly encountered in clinical practice [22]. Together with the lower proportion of DMD sufferers who might potentially have renal involvement [19, 21], it reinforces the need for alternative techniques. TA could initially be part of research assessments and, after further validation and automation, be incorporated gradually into existing routine clinical workflows [37]. Developing a pipeline adapted to specific clinical needs could provide

clinicians with two main benefits: the ability to exploit native CMR examinations for particular patient subgroups when required and the flexibility to extend texture analysis models by integrating relevant clinical data, potentially enabling more advanced applications such as risk stratification tools to improve prognosis in DMD patients. Building on this approach, enhancing non-contrast imaging has the potential to optimize cardiac MRI examinations for DMD patients, improving their disease monitoring while minimizing GBCA use.

Limitations

Our study has limitations. It was retrospectively performed in a single center, so our sample size was small. Additionally, our results were not externally validated, limiting their clinical applicability and generalizability. Nonetheless, the TA approach followed in this study can be extended to other pathologies beyond DMD. Even though more types of texture analysis exist in the literature, our study is based on one that has been consistently applied in cardiac MRI. Likewise, although we minimized patient selection bias, we could not rule it out completely, and we worked with artifact-free images. Even though they might not always represent the clinical practice, it is necessary to ensure the utility of texture features, as artifacts can significantly impact their assessment and compromise their reliability. Finally, even though there are conventional and widely studied clinical markers that predict LGE, we wanted to contribute to understanding how specific features can independently provide insight into LGE in DMD patients to advance knowledge in cardiac imaging. Future research will benefit from collaborative efforts to study the utility of IDMN assessment in DMD patients, establish a direct correlation between T1 mapping-derived TA features and their long-term clinical outcomes, and analyze the feasibility of reducing the frequency of GBCA use during their regular controls.

Conclusion

We successfully implemented a pipeline for extracting texture features from cardiac MRI native T1 mapping and studied their potential in assessing LGE in DMD patients. Our findings showed that IDMN, a feature that measures the homogeneity of pixel values in a region, might aid in detecting slight myocardial tissue alterations associated with LGE, which is crucial for monitoring the cardiovascular health in these patients. Furthermore, IDMN might leverage the information native T1 parametric mapping provides, helping to reduce the use of GBCA in these patients' yearly cardiac MRI examinations and aiding those with difficult venous access.

Abbreviations

AIC	Akaike information criterion
AUC	Area under the curve

BIC	Bayesian information criterion
CI	Confidence interval
CMR	Cardiovascular magnetic resonance
CV	Coefficient of variation
DMD	Duchenne muscular dystrophy
EDV	End-diastolic volume
EF	Ejection fraction
ESV	End-systolic volume
FW	Free wall
GBCA	Gadolinium-based contrast agent
GLCM	Gray-level co-occurrence matrix
GLDM	Gray-level dependence matrix
GLM	Generalized linear mixed
GLRLM	Gray-level run length matrix
GLSZM	Gray-level size-zone matrix
ICC	Intraclass correlation coefficient
IDMN	Inverse difference moment normalized
ISP	Intelli Space Portal
LBP	Local binary pattern
LGE	Late gadolinium enhancement
LV	Left ventricle
LVM	Left ventricular mass
MAPSE	Mitral annular plane systolic excursion
MOLLI	Modified Look-Locker inversion recovery
NGTDM	Neighbouring gray-tone-difference matrix
NifTI	Neuroimaging Informatics Technology Initiative
RMS	Root mean squared
ROC	Receiver operating characteristic
RV	Right ventricle
SSFP	Steady-state free precession
SV	Stroke volume
TA	Texture analysis
TAPSE	Tricuspid annular plane systolic excursion
VIF	Variable inflation factor
WT	Wall thickness

Supplementary Information

The online version contains supplementary material available at <https://doi.org/10.1186/s13023-025-03662-y>.

Supplementary Material 1

Acknowledgements

The authors acknowledge the doctors involved in the Parent Project from the Czech Republic for their initial efforts in gathering the DMD patients and conducting the original study, the radiographers, and Dr. Martina Kelblová for collaborating with clinical analyses.

Author contributions

RP and VF developed the primary project and established the CMR protocol. MLMP and RP conceived the study. RP, VF, and LO oversaw patient inclusion. VF and RP conducted the clinical analyses. MLMP and TH performed the CMR data analyses. MLMP developed the algorithm, performed the statistical analysis, and drafted the manuscript. All authors discussed the results, read and critically reviewed the manuscript, and accepted the final version.

Funding

This study has received funding from the Next Generation EU under the National Institute for Research of Metabolic and Cardiovascular Disease project (Programme EXCELES, ID Project LX22NPO5104) and the Masaryk University under the project "Heart failure, its comorbidities and etiological causes" (MUNI/A/1624/2023).

Data availability

The datasets used and/or analysed during the current study cannot be publicly shared because of patient's privacy but are available from the corresponding author on reasonable request.

Declarations

Ethics approval and consent to participate

Institutional Review Board approval was not required because the data used in this study were retrospectively gathered from patients who had previously participated in a research study approved by the institutional Ethics Committee at the University Hospital Brno (reference number 20130410-03) under the Declaration of Helsinki (2000) of the World Medical Association.

Consent for publication

Not applicable.

Competing interests

The authors declare that they have no competing interests.

Received: 14 November 2024 / Accepted: 8 March 2025

Published online: 19 March 2025

References

- Duan D, Goemans N, Takeda Si, Mercuri E, Aartsma-Rus A. Duchenne muscular dystrophy. *Nat Reviews Disease Primers*. 2021;7(1):13.
- Birnkrant DJ, Bushby K, Bann CM, Alman BA, Apkon SD, Blackwell A, et al. Diagnosis and management of Duchenne muscular dystrophy, part 2: respiratory, cardiac, bone health, and orthopaedic management. *Lancet Neurol*. 2018;17(4):347–61.
- Buddhe S, Cripe L, Friedland-Little J, Kertesz N, Eghtesady P, Finder J, et al. Cardiac management of the patient with Duchenne muscular dystrophy. *Pediatrics*. 2018;142(Suppl 2):S72–81.
- Feingold B, Mahle WT, Auerbach S, Clemens P, Domenighetti AA, Jefferies JL, et al. Management of cardiac involvement associated with neuromuscular diseases: A scientific statement from the American heart association. *Circulation*. 2017;136(13):e200–31.
- Haaf P, Garg P, Messroghli DR, Broadbent DA, Greenwood JP, Plein S. Cardiac T1 mapping and extracellular volume (ECV) in clinical practice: a comprehensive review. *J Cardiovasc Magn Reson*. 2016;18(1):89.
- Taylor AJ, Salerno M, Dharmakumar R, Jerosch-Herold M. T1 mapping: basic techniques and clinical applications. *JACC: Cardiovasc Imaging*. 2016;9(1):67–81.
- Puntmann VO, Valbuena S, Hinojar R, Petersen SE, Greenwood JP, Kramer CM, et al. Society for cardiovascular magnetic resonance (SCMR) expert consensus for CMR imaging endpoints in clinical research: part I - analytical validation and clinical qualification. *J Cardiovasc Magn Reson*. 2018;20(1):67.
- Flett AS, Hasleton J, Cook C, Hausenloy D, Quarta G, Ariti C, et al. Evaluation of techniques for the quantification of myocardial Scar of differing etiology using cardiac magnetic resonance. *JACC: Cardiovasc Imaging*. 2011;4(2):150–6.
- Guo BJ, Yang ZL, Zhang LJ. Gadolinium deposition in brain: current scientific evidence and future perspectives. *Front Mol Neurosci*. 2018;11:335.
- McDonald RJ, McDonald JS, Kallmes DF, Jentoft ME, Murray DL, Thielen KR, et al. Intracranial gadolinium deposition after Contrast-enhanced. *MR Imaging*. 2015;27(3):772–82.
- Zaki N, Parra D, Wells Q, Chew JD, George-Durrett K, Pruthi S, Soslow J. Assessment of gadolinium deposition in the brain tissue of pediatric and adult congenital heart disease patients after contrast enhanced cardiovascular magnetic resonance. *J Cardiovasc Magn Reson: Official J Soc Cardiovasc Magn Reson*. 2020;22(1):82.
- Valsangiacomo Buechel ER, Grosse-Wortmann L, Fratz S, Eichhorn J, Sarikouch S, Greil GF, et al. Indications for cardiovascular magnetic resonance in children with congenital and acquired heart disease: an expert consensus paper of the imaging working group of the AEPCC and the cardiovascular magnetic resonance section of the EACVI. *Eur Heart J - Cardiovasc Imaging*. 2015;16(3):281–97.
- Kali A, Cokic I, Tang RL, Yang HJ, Sharif B, Marbán E, et al. Determination of location, size, and transmural of chronic myocardial infarction without exogenous contrast media by using cardiac magnetic resonance imaging at 3 T. *Circ Cardiovasc Imaging*. 2014;7(3):471–81.
- Ozkok SO, Abdullah. Contrast-induced acute kidney injury: A review of practical points. *World J Nephrol*. 2017;6(3):14.

15. Le Fur M, Caravan P. The biological fate of gadolinium-based MRI contrast agents: a call to action for bioinorganic chemists. *Metallomics*. 2019;11(2):240–54.
16. Ramalho J, Semelka RC, Ramalho M, Nunes RH, AlObaidy M, Castillo M. Gadolinium-Based contrast agent accumulation and toxicity: an update. *AJNR Am J Neuroradiol*. 2016;37(7):1192–8.
17. Bruder O, Schneider S, Nothnagel D, Pilz G, Lombardi M, Sinha A, et al. Acute adverse reactions to Gadolinium-Based contrast agents in CMR: multicenter experience with 17,767 patients from the EuroCMR registry. *JACC: Cardiovasc Imaging*. 2011;4(11):1171–6.
18. Raucci FJ, Xu M, George-Durrett K, Crum K, Slaughter JC, Parra DA, et al. Non-contrast cardiovascular magnetic resonance detection of myocardial fibrosis in Duchenne muscular dystrophy. *J Cardiovasc Magn Reson*. 2021;23(1):48.
19. Kutluk MG, Doğan ÇS. Kidney involvement and associated risk factors in children with Duchenne muscular dystrophy. *Pediatr Nephrol*. 2020;35(10):1953–8.
20. Lang SM, Alsaied T, Moore RA, Rattan M, Ryan TD, Taylor MD. Conservative gadolinium administration to patients with Duchenne muscular dystrophy: decreasing exposure, cost, and time, without change in medical management. *Int J Cardiovasc Imaging*. 2019;35(12):2213–9.
21. Motoki T, Shimizu-Motohashi Y, Saito I, Komaki H, Ishiyama A, Aibara K, et al. Renal dysfunction can occur in advanced-stage Duchenne muscular dystrophy. *Muscle Nerve*. 2020;61(2):192–7.
22. Ng M, Mark LKF, Fatimah L. Management of difficult intravenous access: a qualitative review. *World J Emerg Med*. 2022;13(6):467–78.
23. Zhang Q, Burrage MK, Shanmuganathan M, Gonzales RA, Lukaschuk E, Thomas KE, et al. Artificial intelligence for Contrast-Free MRI: Scar assessment in myocardial infarction using deep Learning-Based virtual native enhancement. *Circulation*. 2022;146(20):1492–503.
24. Castellano G, Bonilha L, Li LM, Cendes F. Texture analysis of medical images. *Clin Radiol*. 2004;59(12):1061–9.
25. Hassani C, Saremi F, Varghese BA, Duddalwar V. Myocard Radiomics Cardiac MRI. 2020;214(3):536–45.
26. MacKay JW, Murray PJ, Kasmai B, Johnson G, Donell ST, Toms AP. MRI texture analysis of subchondral bone at the tibial plateau. *Eur Radiol*. 2016;26(9):3034–45.
27. Huang S, Shi K, Zhang Y, Yan W-F, Guo Y-K, Li Y, Yang Z-G. Texture analysis of T2-weighted cardiovascular magnetic resonance imaging to discriminate between cardiac amyloidosis and hypertrophic cardiomyopathy. *BMC Cardiovasc Disord*. 2022;22(1):235.
28. Baessler B, Luecke C, Lurz J, Klingel K, Roeder Mv W, Sd et al. Cardiac MRI texture analysis of T1 and T2 maps in patients with infarctlike acute myocarditis. *Radiology*. 2018;289(2):357–65.
29. Antonopoulos AS, Boutsikou M, Simantiris S, Angelopoulos A, Lazaros G, Panagiotopoulos I, et al. Machine learning of native T1 mapping radiomics for classification of hypertrophic cardiomyopathy phenotypes. *Sci Rep*. 2021;11(1):23596.
30. Cheng S, Fang M, Cui C, Chen X, Yin G, Prasad SK, et al. LGE-CMR-derived texture features reflect poor prognosis in hypertrophic cardiomyopathy patients with systolic dysfunction: preliminary results. *Eur Radiol*. 2018;28(11):4615–24.
31. Marfisi D, Tessa C, Marzi C, Del Meglio J, Linsalata S, Borgheresi R, et al. Image resampling and discretization effect on the estimate of myocardial radiomic features from T1 and T2 mapping in hypertrophic cardiomyopathy. *Sci Rep*. 2022;12(1):10186.
32. Neisius U, El-Rewaify H, Kucukseymen S, Tsao CW, Mancio J, Nakamori S et al. Texture signatures of native myocardial T1 as novel imaging markers for identification of hypertrophic cardiomyopathy patients without scar. *J Magn Reson Imaging*. 2020;52(3):906–19.
33. Shao X-N, Sun Y-J, Xiao K-T, Zhang Y, Zhang W-B, Kou Z-F, Cheng J-L. Texture analysis of magnetic resonance T1 mapping with dilated cardiomyopathy: A machine learning approach. *Medicine (Baltimore)*. 2018;97(37):e12246.
34. Baessler B, Luecke C, Lurz J, Klingel K, Das A, von Roeder M et al. Cardiac MRI and texture analysis of myocardial T1 and T2 maps in myocarditis with acute versus chronic symptoms of heart failure. *Radiology*. 2019;292(3):608–17.
35. Peng F, Zheng T, Tang X, Liu Q, Sun Z, Feng Z, et al. Magnetic resonance texture analysis in myocardial infarction. *Front Cardiovasc Med*. 2021;8:724271.
36. Mannil M, Kato K, Manka R, von Spiczak J, Peters B, Cammann VL, et al. Prognostic value of texture analysis from cardiac magnetic resonance imaging in patients with Takotsubo syndrome: a machine learning based proof-of-principle approach. *Sci Rep*. 2020;10(1):20537.
37. Raisi-Estabragh Z, Izquierdo C, Campello VM, Martin-Isla C, Jaggi A, Harvey NC, et al. Cardiac magnetic resonance radiomics: basic principles and clinical perspectives. *Eur Heart J Cardiovasc Imaging*. 2020;21(4):349–56.
38. Ho DE, Imai K, King G, Stuart EA. MatchIt: nonparametric preprocessing for parametric causal inference. *J Stat Softw*. 2011;42(8):1–28.
39. Hansen BB. Full matching in an observational study of coaching for the SAT. *J Am Stat Assoc*. 2004;99(467):609–18.
40. Parent Project Czech Republic. [Available from: <https://www.parentproject.cz>
41. Stehlíková K, Skálová D, Zídková J, Haberlová J, Vohánka S, Mazanec R et al. Muscular dystrophies and myopathies: the spectrum of mutated genes in the Czech Republic. *Clin Genet*. 2017;91(3):463–9.
42. Vry J, Gramsch K, Rodger S, Thompson R, Steffensen BF, Rahbek J, et al. European Cross-Sectional Survey of Current Care Practices for Duchenne Muscular Dystrophy Reveals Regional and Age-Dependent Differences. *Journal of Neuromuscular Diseases*. 2016;3:517–27.
43. Panovský R, Peší M, Holeček T, Máchal J, Feitová V, Mrázová L, et al. Cardiac profile of the Czech population of Duchenne muscular dystrophy patients: a cardiovascular magnetic resonance study with T1 mapping. *Orphanet J Rare Dis*. 2019;14(1):10.
44. Panovský R, Peší M, Máchal J, Holeček T, Feitová V, Juříková L, et al. Quantitative assessment of left ventricular longitudinal function and myocardial deformation in Duchenne muscular dystrophy patients. *Orphanet J Rare Dis*. 2021;16(1):57.
45. Schulz-Menger J, Bluemke DA, Bremerich J, Flamm SD, Fogel MA, Friedrich MG, et al. Standardized image interpretation and post-processing in cardiovascular magnetic resonance—2020 update. *J Cardiovasc Magn Reson*. 2020;22(1):19.
46. van Griethuysen JJM, Fedorov A, Parmar C, Hosny A, Aucoin N, Narayan V, et al. Computational radiomics system to Decode the radiographic phenotype. *Cancer Res*. 2017;77(21):e104–7.
47. Collewet G, Strzelecki M, Mariette F. Influence of MRI acquisition protocols and image intensity normalization methods on texture classification. *Magn Reson Imaging*. 2004;22(1):81–91.
48. Baeßler B, Mannil M, Maintz D, Alkadhi H, Manka R. Texture analysis and machine learning of non-contrast T1-weighted MR images in patients with hypertrophic cardiomyopathy—Preliminary results. *Eur J Radiol*. 2018;102:61–7.
49. Kursa MB, Rudnicki WR. Feature selection with the Boruta package. *J Stat Softw*. 2010;36(11):1–13.
50. Tibshirani R. Regression shrinkage and selection via the Lasso: A retrospective. *J Royal Stat Soc Ser B: Stat Methodol*. 2011;73(3):273–82.
51. Koo TK, Li MY. A guideline of selecting and reporting intraclass correlation coefficients for reliability research. *J Chiropr Med*. 2016;15(2):155–63.
52. R Core Team. R: A Language and environment for statistical computing. Vienna, Austria: R Foundation for Statistical Computing; 2023.
53. Kosmidis I, Firth D. Jeffreys-prior penalty, finiteness and shrinkage in binomial-response generalized linear models. *Biometrika*. 2021;108(1):71–82.
54. Kuhn M. Building predictive models in R using the caret package. *J Stat Softw*. 2008;28(5):1–26.
55. Friedman J, Tibshirani R, Hastie T. Regularization paths for generalized linear models via coordinate descent. *J Stat Softw*. 2010;33(1):1–22.
56. Tay JK, Narasimhan B, Hastie T. Elastic net regularization paths for all generalized linear models. *J Stat Softw*. 2023;106(1):1–31.
57. Wolak ME, Fairbairn DJ, Paulsen YR. Guidelines for estimating repeatability. *Methods Ecol Evol*. 2012;3(1):129–37.
58. Robin X, Turck N, Hainard A, Tiberti N, Lisacek F, Sanchez J-C, Müller M. pROC: an open-source package for R and S+ to analyze and compare ROC curves. *BMC Bioinformatics*. 2011;12:77.
59. El-Rewaify H, Neisius U, Nakamori S, Ngo L, Rodriguez J, Manning WJ, Nezafat R. Characterization of interstitial diffuse fibrosis patterns using texture analysis of myocardial native T1 mapping. *PLoS ONE*. 2020;15(6):e0233694.
60. Mafoor NG, Magrath P, Moulin K, Shao J, Kim GH, Prosper A, et al. T1-Mapping and extracellular volume estimates in pediatric subjects with Duchenne muscular dystrophy and healthy controls at 3T. *J Cardiovasc Magn Reson*. 2020;22(1):85.
61. Olivieri LJ, Kellman P, McCarter RJ, Cross RR, Hansen MS, Spurney CF. Native T1 values identify myocardial changes and stratify disease severity in patients with Duchenne muscular dystrophy. *J Cardiovasc Magn Reson*. 2016;18(1):72.
62. Soslow JH, Damon SM, Crum K, Lawson MA, Slaughter JC, Xu M, et al. Increased myocardial native T1 and extracellular volume in patients with Duchenne muscular dystrophy. *J Cardiovasc Magn Reson*. 2016;18(1):5.

63. Xu K, Xu H-y, Xu R, Xie L-j, Yang Z-g, Yu L, et al. Global, segmental and layer specific analysis of myocardial involvement in Duchenne muscular dystrophy by cardiovascular magnetic resonance native T1 mapping. *J Cardiovasc Magn Reson*. 2021;23(1):110.
64. Lang SM, Alsaied T, Khoury PR, Ryan TD, Taylor MD. Variations in native T1 values in patients with Duchenne muscular dystrophy with and without late gadolinium enhancement. *Int J Cardiovasc Imaging*. 2021;37(2):635–42.
65. Hor KN, Taylor MD, Al-Khalidi HR, Cripe LH, Raman SV, Jefferies JL, et al. Prevalence and distribution of late gadolinium enhancement in a large

population of patients with Duchenne muscular dystrophy: effect of age and left ventricular systolic function. *J Cardiovasc Magn Reson*. 2013;15(1):107.

Publisher's note

Springer Nature remains neutral with regard to jurisdictional claims in published maps and institutional affiliations.